Pergamon

Environment International, Vol. 23, No. 6, pp. 839–850, 1997

0160-4120/97 $17.00+.00

PII S0160-4120(97)00096-2

A MODEL FOR THE PREDICTION OF OIL SLICK MOVEMENT AND SPREADING USING CELLULAR AUTOMATA

Ioannis Karafyllidis
Democritus University of Thrace, Department of Electrical and Computer Engineering, GR-671 00 Xanthi, Greece

EI 9702-112 M (Received 1 February 1997; accepted 16 June 1997)

A model for the prediction of oil slick movement and spreading, using Cellular Automata, is presented in this paper. The model is general and can predict the behaviour of oil slicks in regions with complicated boundaries. The effects of winds, surface currents, and oil evaporation have been taken into account. An algorithm for the simulation of oil slick movement and spreading, based on this model, has also been developed and has been used to simulate hypothetical oil slicks in hypothetical geographical regions. The results of the simulation are in qualitative agreement with real oil slick movement and spreading. ©1997 Elsevier Science Ltd

INTRODUCTION

Extensive oil drilling and transportation activities increase the possibility of oil spills and the consequent threat of oil pollution to the regional environment. Oil spills are hazards for marine and freshwater environments and oil spill/slick detection, monitoring, and management has received considerable attention over the past few years (Cunningham and Saigo 1995). Oil slicks are detected and quantified, and their movement is monitored using satellites (Ages et al. 1994; MacDonald et al. 1993; Massin 1984; Okamoto et al. 1994), airborne systems (Gruner et al. 1991; Krapez and Cielo 1992), and radars (Bass and Puzenko 1994; Huhnerfuss et al. 1989).

One of the major problems in oil slick combat and management is the prediction of the behaviour (movement and spreading) of oil slicks. Generally, the goal of predicting the behaviour of oil slicks is the determination of the time-evolving shape of the slick under various weather conditions, in waters where currents exist. Wind direction and speed are the most important weather conditions. Although great progress has been made in detecting and monitoring oil slicks, a general model for oil slick movement and spreading has not been yet devised (Neralla and Venkatesh 1989; Easton 1989; Adam 1995). Models for oil slick behaviour are important in environmental engineering and are used as decision support systems in environmental emergency response (Lehr et al. 1994). These models are also used to help ships avoid oil slicks (Adam 1995).

Several models for the prediction of the behaviour of oil slicks have been developed. One of the major difficulties in oil slick modelling is the complex shape of the coasts which impose the boundary conditions on the problem. Because of this difficulty, most of these models have been developed to predict oil slick behaviour in particular geographical regions, namely in Florida waters (Cekirge et al. 1990), in the Florida Gulf (Capehart and Welsh 1978; 1979), in Puget Sound (Karpen and Galt 1979), in the St. Laurence River (Yapa et al. 1992), in the lakes of the Mackenzie River (Phillips and Groseva 1977), in Spencer Gulf (Beer et al. 1983), in Bombay (Gouveia and Kurup 1977), and in the Arabian Gulf and Sea (El-sabh and Murty 1988; Kurup 1983).

Artificial oil slicks have been created and observed in order to construct semi-empirical models for oil slick motion and spreading (Alofs and Reisbig 1972; Neralla and Venkatesh 1989; Okuyama et al. 1988). Attempts have been made to describe oil slick behaviour using hydrodynamical equations (Cekirge et al. 1990) and a Lagrangian-Eulerian model (Karpen and Galt 1979), but, in both cases, surface currents and winds have not been taken into account.

The problem of predicting oil slick movement and spreading is a highly non-linear problem and the shape of coasts and islands impose complicated boundary conditions. Oil slicks move under the influence of winds and surface currents and, furthermore, oil slicks diffuse horizontally and oil evaporates (Reijnhart and Rose 1982). It is difficult to describe the action of all these parameters using Partial Differential Equations (PDEs). Such an attempt will probably lead to a system of PDEs which will be difficult to handle. Cellular Automata (CAs) are an alternative to PDEs and have been used successfully in modelling physical systems and processes (Toffoli 1984a; Omohundro 1984). The aim of this work is to develop an initial form of a general model for oil slick movement and spreading using CAs.

In the framework of this research work, a model for the prediction of oil slick movement and spreading has been developed. The model is general and can predict the behaviour of oil slicks in regions with complicated boundaries. The effects of winds, surface currents, and oil evaporation have been taken into account. An algorithm for the simulation of oil slick movement and spreading, based on this model, has also been developed. The algorithm has been used to simulate hypothetical oil slick movement and spreading in hypothetical geographical regions. The results of the simulation are in qualitative agreement with real oil slick movement and spreading.

CELLULAR AUTOMATA

CAs are models of physical systems where space and time are discrete and interactions only local. CAs, first introduced by von Neumann (von Neumann 1966), have been extensively used as models for complex systems (Wolfram 1994). CAs have also been applied to several physical problems, where local interactions are involved (Gerhard and Schuster 1989; Gerhard et al. 1990; Weimar et al. 1992; Karafyllidis and Thanailakis 1995, 1996). In spite of the simplicity of their structure, CAs exhibit complex dynamical behaviour and can describe many physical systems and processes. A Cellular Automaton (CA) consists of a regular uniform n-dimensional lattice (or array). At each site of the lattice (cell) a physical quantity takes values. This physical quantity is the global state of the CA, and the value of this quantity at each cell is the local state of this cell. Each cell is restricted to local neighbourhood interaction only, and, as a result, it is incapable of immediate global communication (von Neumann 1966). The neighbourhood of a cell is taken to be the cell itself and some (or all) of the immediately adjacent and diagonal cells. The states at each cell are updated simultaneously at discrete time steps, based on the states in their neighbourhood at the preceding time step. The algorithm used to compute the next cell state is referred to as the CA local rule. Usually the same local rule applies to all cells of the CA.

A CA is characterised by five properties:

1) the number of spatial dimensions (n);
2) the width of each side of the array (w). w_j is the width of the jth side of the array, where j=1,2,3,...n;
3) the width of the neighbourhood of the cell (d). d_j is the width of the neighbourhood at the jth side of the array;
4) the state of the CA cells; and
5) the CA local rule, which is an arbitrary function F.

The state of a cell at time step (t+1) is computed according to F. F is a function of the state of this cell and of the states of the cells in its neighbourhood at time step (t). The case of a two-dimensional CA (n=2), with neighbourhood width d_1=3 and d_2=3, is shown in Fig. 1. In this case, the neighbourhood of the (i,j) cell consists of the same cell and of all eight cells which are adjacent and diagonal to it. The CA local rule, which calculates the state of the (i,j) cell at time step t+1, is a function of the (i,j) cell's own state and of the states of all eight cells in its neighbourhood at time step t:

$$C^{t+1}_{i,j} = F\,(C^t_{i-1,j-1}, C^t_{i-1,j}, C^t_{i-1,j+1}, C^t_{i,j-1}, C^t_{i,j}, C^t_{i,j+1}, C^t_{i+1,j-1}, C^t_{i+1,j}, C^t_{i+1,j+1}) \quad (1)$$

$C^t_{i,j}$ and $C^{t+1}_{i,j}$ are the states of the (i,j) cell at time steps t and t+1, respectively.

CAs have enough expressive power to represent phenomena of arbitrary complexity and, at the same time, they can be simulated exactly by digital computers because of their intrinsic discreteness, i.e., the topology of the simulated object is reproduced in the simulating device (Vichniac 1984; Wilding et al. 1991).

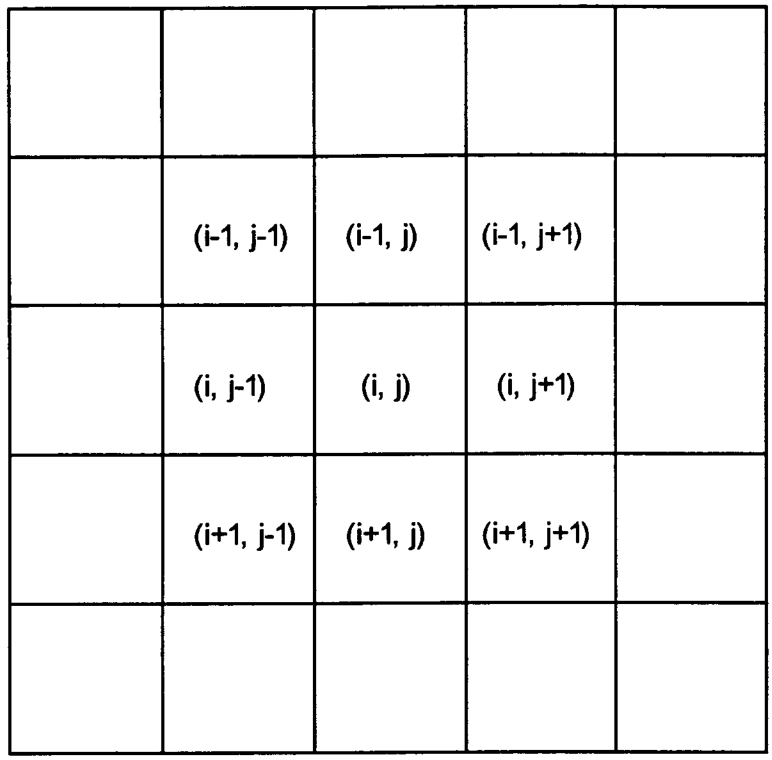

Fig. 1. The neighbourhood of the (i,j) cell is formed by the same (i,j) cell and the eight marked cells.

Mathematical tools for simulating physics, namely PDEs, contain much more information than is usually needed, because variables take an infinite number of values in a continuous space. PDEs are used to compute values of physical quantities at points in continuous time. But the values of physical quantities are usually measured over finite areas or volumes at discrete time steps (Toffoli 1984a). CAs are used to compute values of physical quantities over finite areas (CA cells) at discrete time steps. The CA approach is consistent with the modern notion of unified space-time where space (memory, i.e., CA cell state) and time (processing unit, i.e., CA local rule) are inseparable, i.e., located to a CA cell (Matzke 1994; Omtzigt 1994). Because of the above reasons, algorithms based on CAs run fast on digital computers (Toffoli 1984a; Matzke 1994). More about modelling physics with CA may be found in Vichniac (1984), Minsky (1982), Feynman (1982), and Zeigler (1982).

Models based on CAs lead to algorithms which are fast when implemented on serial computers because they exploit the inherent parallelism of the CA structure. These algorithms are also appropriate for implementation on massively parallel computers, such as CAM (Wilding et al. 1991; Toffoli 1984b).

DESCRIPTION OF THE MODEL

In order to model oil slick movement and spreading, the surface of the area where the spill occurred is divided into a matrix of identical square cells, with side length a, and it is represented by a CA by assuming that each square cell of the surface is a CA cell. This area includes water (sea, lake, river) areas and land (coasts, islands) areas.

The number of spatial dimensions of the CA is: n=2.

The widths of the two sides of the CA are taken to be equal, i.e., $w_1=w_2$.

The width of the neighbourhood of the (i,j) cell is taken to be equal to three at both sides, i.e., $d_1=d_2=3$. Figure 1 shows the neighbourhood of the (i,j) cell.

The state of the (i,j) cell at time t, $C^t_{i,j}$, is:

$$C^t_{i,j} = \{LF, M^t_{i,j}, CD^t_{i,j}, CV^t_{i,j}, WD^t_{i,j}, WV^t_{i,j}\} \quad (2)$$

LF is a one bit flag which indicates land or water areas. If the (i,j) cell is a land area, then LF=1, whereas, if the (i,j) cell is a water area, LF=0. $M^t_{i,j}$ is the oil mass at time t in the area corresponding to the (i,j) cell. $CV^t_{i,j}$ and $WV^t_{i,j}$ are the water current and wind speeds at time t in the area corresponding to the

(i,j) cell, respectively. $CD^t_{i,j}$ and $WD^t_{i,j}$ are flags that indicate the direction of the current and wind speed at time t in the area corresponding to the (i,j) cell, respectively. The number of bits in these flags is proportional to the number of directions, i.e., if the number of bits is two, then the flags can indicate only four directions: 00 corresponds to north direction; 01 corresponds to east direction; 10 corresponds to south direction; and 11 corresponds to west direction.
If the number of bits is three, then the flags can indicate eight directions:

000 : north direction
001 : north-east direction
010 : east direction
011 : south-east direction
100 : south direction; (3)
101 : south-west direction
110 : west direction
111 : north-west direction

The values of LF, $CD^t_{i,j}$, $CV^t_{i,j}$, $WD^t_{i,j}$ and $WV^t_{i,j}$ are the inputs to the model, i.e., the geography (LF), the wind direction and speed ($WD^t_{i,j}$, $WV^t_{i,j}$) at all times, and the water current direction and speed ($CD^t_{i,j}$ and $CV^t_{i,j}$) at all times are not calculated in this model, but assumed to be given by some other simulation (weather or surface current simulation) or system. The initial distribution of oil mass in the cells ($M^0_{i,j}$) is also an input to the model. The problem of predicting the oil slick movement and spreading is stated as follows: Given the oil mass distribution at time t=0 (i.e., $M^0_{i,j}$), the geography, the wind and water current speed and direction, determine the oil mass distribution at all future times t > 0 (i.e., $M^t_{i,j}$).

Figure 2 shows the neighbourhood of the (i,j) cell and the oil masses in each cell at time t. Generally, the oil masses are not equal to each other and therefore oil is transported from cells where oil mass is large to cells where oil mass is small. The driving force for oil transport between two cells is the difference of oil mass. Consider the (i,j) cell and one of its neighbours, the (i-1,j) cell. If at time t $M^t_{i,j} > M^t_{i-1,j}$, then at time t+1, oil will be transported from the (i,j) cell to the (i-1,j) cell, whereas, if $M^t_{i,j} < M^t_{i-1,j}$, then at time t+1, oil will be transported from the (i-1,j) cell to the (i,j) cell. As a first order approximation, the transported oil mass is supposed to be proportional to the oil mass difference between the two cells. The oil mass in cell (i,j) at time t+1 is given by:

$M^t_{i-1,j-1}$	$M^t_{i-1,j}$	$M^t_{i-1,j+1}$
$M^t_{i,j-1}$	$M^t_{i,j}$	$M^t_{i,j+1}$
$M^t_{i+1,j-1}$	$M^t_{i+1,j}$	$M^t_{i+1,j+1}$

Fig. 2. The neighbourhood of the (i,j) cell and the oil masses in each cell at time t.

$$M^{t+1}_{i,j} = M^t_{i,j} + m(M^t_{i-1,j} - M^t_{i,j}) \tag{4}$$

where m is constant. The value of this constant will be determined in the next section. Equation 4 describes the change of oil mass in the (i,j) cell because of oil transport to or from the (i-1,j) cell. Equation 4 may be used to determine the oil mass change in the (i,j) cell because of oil transport to or from the four adjacent cells. Obviously, oil transport between diagonal cells is less than oil transport between adjacent cells. The change of oil mass in the (i,j) cell due to transport from (to) the (i,j) cell to (from) one of its diagonal cells (for example, the (i-1,j-1) cell) is given by:

$$M^{t+1}_{i,j} = M^t_{i,j} + m(d(M^t_{i-1,j-1} - M^t_{i,j})) \tag{5}$$

d is a constant which absorbs the difference between oil transport between diagonal cells and oil transport between adjacent cells. The value of this constant will be determined in the next section. When oil transport to or from all eight neighbouring cells is taken into account, the oil mass in the (i,j) cell at time t+1 is given by:

$$\begin{aligned} M^{t+1}_{i,j} = M^t_{i,j} &+ m[(M^t_{i-1,j} - M^t_{i,j}) + (M^t_{i+1,j} - M^t_{i,j}) \\ &+ (M^t_{i,j-1} - M^t_{i,j}) + (M^t_{i,j+1} - M^t_{i,j})] \\ &+ m\,d[(M^t_{i-1,j-1} - M^t_{i,j}) + (M^t_{i+1,j-1} - M^t_{i,j}) \\ &+ (M^t_{i-1,j+1} - M^t_{i,j}) + (M^t_{i+1,j+1} - M^t_{i,j})] \end{aligned} \tag{6}$$

Equation 6 preserves the total oil mass because the oil mass transported into the (i,j) cell from some other cell, the (i+1,j) cell, is equal to the oil mass transported out of the (i+1,j) cell. If one of the neighbouring cells is a land area (i.e. LF=1), then it is assumed that no oil transport is possible to or from that cell and the corresponding term in Eq. 6 is not taken into account.

In an oil slick, oil mass is continuously reduced because of oil evaporation. Considering a standard surface, i.e., the CA cell, the oil evaporation rate depends mainly on temperature (Reijnhart and Rose 1982). In order to include oil evaporation, another term has been added to Eq. 6:

$$\begin{aligned} M^{t+1}_{i,j} = M^t_{i,j} &+ m[(M^t_{i-1,j} - M^t_{i,j}) + (M^t_{i+1,j} - M^t_{i,j}) \\ &+ (M^t_{i,j-1} - M^t_{i,j}) + (M^t_{i,j+1} - M^t_{i,j})] \\ &+ m\, d[(M^t_{i-1,j-1} - M^t_{i,j}) + (M^t_{i+1,j-1} - M^t_{i,j}) \\ &+ (M^t_{i-1,j+1} - M^t_{i,j}) + (M^t_{i+1,j+1} - M^t_{i,j})] - p\, t_m\, T^t \end{aligned} \tag{7}$$

The term ($p\, t_m\, T^t$) is a first order approximation for the oil evaporation rate, i.e., the oil mass evaporated during a time step (Reijnhart and Rose 1982). Constant p is a user defined constant with units [kg (sec K)$^{-1}$], t_m is the time corresponding to a model time step and T^t is the temperature of the environment at time step t (t in T^t is an index and not an exponent).

Equation 7 describes the simultaneous spreading and evaporation of oil slicks when no winds blow and no water currents are present. Winds generate temporary water currents, which are called wind-driven currents (Phillips and Groseva 1977).

Water currents and wind-driven currents greatly affect oil transport from one cell to another. Suppose that the CA array is oriented in such a way that the (i-1,j) cell is located to the north of the (i,j) cell, the (i,j-1) cell to the west, the (i+1,j) cell to the south, and the (i,j+1) cell to the east. Suppose that a current (water or wind-driven) flows from west to east. This current will enhance oil transport from west to east, i.e., from the (i,j-1) cell to the (i,j) cell and from the (i,j) cell to the (i,j+1) cell, and will reduce oil transport from east to west.

If $M^t_{i,j-1} > M^t_{i,j} > M^t_{i,j+1}$ and no currents exist, oil is transported from west to east because of the oil mass differences. If only these three cells are taken into account, then according to Eq. 7, the oil mass in the (i,j) cell at time step t+1 is given by:

$$M^{t+1}_{i,j} = M^t_{i,j} + m[(M^t_{i,j-1} - M^t_{i,j}) + (M^t_{i,j+1} - M^t_{i,j})] - p\, t_m\, T^t \tag{8}$$

Suppose that a current flows from west to east. This current will enhance the oil transport. In order to model the effect of this current, Eq. 8 is written as follows:

$$\begin{aligned} M^{t+1}_{i,j} = M^t_{i,j} &+ m[((1 + W^t_{i,j})\, M^t_{i,j-1} - M^t_{i,j}) \\ &+ ((1 + E^t_{i,j})\, M^t_{i,j+1} - M^t_{i,j})] - p\, t_m\, T^t \end{aligned} \tag{9}$$

$W^t_{i,j}$ and $E^t_{i,j}$ are constants which are equal to zero when no current exists at time step t at the (i,j) cell. In the case of a current flowing from west to east, the value of the constant $W^t_{i,j}$ is greater than zero and the value of $E^t_{i,j}$ is less than zero. Therefore, $(1+ W^t_{i,j}) > 1$ and the mass difference between cells (i,j-1) and (i,j) increases and, consequently, oil transport from the (i,j-1) cell to the (i,j) cell is enhanced. Constant $E^t_{i,j}$ is less than zero and therefore $(1+E^t_{i,j}) < 1$. Since $M^t_{i,j} > M^t_{i,j+1}$, the mass difference between cells (i,j) and (i,j+1) increases and oil transport from the (i,j) cell to the (i,j+1) cell is also enhanced. The absolute values of $W^t_{i,j}$ and $E^t_{i,j}$ depend on the current speed as it will be explained later in this section.

If $M^t_{i,j-1} < M^t_{i,j} > M^t_{i,j+1}$ and no currents exist, oil is transported from the (i,j) cell to the two neighbouring cells. Suppose again that a current flows from west to east. As in the previous case, the value of the constant $W^t_{i,j}$ is greater than zero and the value of $E^t_{i,j}$ is less than zero.

Since $(1+W^t_{i,j}) > 1$ and $M^t_{i,j-1} < M^t_{i,j}$, the mass difference between cells (i,j-1) and (i,j) is reduced resulting in reduction of oil transport from the (i,j) cell to the (i,j-1) cell. The stronger the current, the larger the absolute value of $W^t_{i,j}$. If the current is strong enough, then it is possible that $(1+W^t_{i,j})\, M^t_{i,j-1} > M^t_{i,j}$, thus reversing the oil transport direction. In order to include the effect of currents in oil transport, Eq. 7 is written as follows:

$$M^{t+1}_{i,j} = M^t_{i,j} + m[((1 + N^t_{i,j})\, M^t_{i-1,j} - M^t_{i,j})$$
$$+ ((1 + S^t_{i,j})\, M^t_{i+1,j} - M^t_{i,j})]$$
$$+ m[((1 + W^t_{i,j})\, M^t_{i,j-1} - M^t_{i,j})$$
$$+ ((1 + E^t_{i,j})\, M^t_{i,j+1} - M^t_{i,j})]$$
$$+ m\, d[((1 + NW^t_{i,j})\, M^t_{i-1,j-1} - M^t_{i,j})$$
$$+ ((1 + SW^t_{i,j})\, M^t_{i+1,j-1} - M^t_{i,j})]$$
$$+ m\, d[((1 + NE^t_{i,j})\, M^t_{i-1,j+1} - M^t_{i,j})$$
$$+ ((1 + SE^t_{i,j})\, M^t_{i+1,j+1} - M^t_{i,j})] - p\, t_m\, T^t \quad (10)$$

Constants $N^t_{i,j}$, $E^t_{i,j}$, $S^t_{i,j}$, $W^t_{i,j}$, $NE^t_{i,j}$, $NW^t_{i,j}$, $SE^t_{i,j}$, and $SW^t_{i,j}$ correspond to north, east, south, west, north-east, north-west, south-east, and south-west directions and are called direction constants. When a current flows from direction X to direction Y, then the constant corresponding to direction X is positive and the constant corresponding to direction Y is negative. The current is modelled more accurately if the values of the constants corresponding to left and right directions of direction X, are also positive but smaller than the constant corresponding to direction X, and if the values of the constants corresponding to left and right directions of direction Y, are also negative but greater than the constant corresponding to direction Y. For example, if a current flows from north to south, the values of the constants are (indices are omitted):

$$N > NE = NW > 0$$
$$W = E = 0$$
$$S < SE = SW < 0$$

Each direction constant models the effect of both water currents and wind-driven currents. The north direction constant is given by:

$$N^t_{i,j} = Nw^t_{i,j} + Nc^t_{i,j} \quad (11)$$

$Nw^t_{i,j}$ models the wind-driven current and is called wind direction constant, whereas $Nc^t_{i,j}$ models the effect of the water current and is called water current direction constant. Equation 11 gives the north direction constant. All the other constants are given by similar equations. The signs of the wind and water current direction constants are determined by the values of $WD^t_{i,j}$ and $CD^t_{i,j}$ which indicate the wind and current direction at time step t, respectively. Therefore, Eq. 10 includes the effects of wind-driven currents and water currents which at time step t have different directions.

In this model, as a first order approximation, the absolute values of wind and water direction constants are taken to be equal to the normalised values of wind and water current speeds:

$$\left| Nw^t_{i,j} \right| = R\frac{WV^t_{i,j}}{WV_{max}} \qquad \left| Nc^t_{i,j} \right| = \frac{CV^t_{i,j}}{CV_{max}} \quad (12)$$

$WV^t_{i,j}$ and $CV^t_{i,j}$ are the wind and current speeds in the (i,j) cell at time step t, respectively. WV_{max} and CV_{max} are the maximum wind and current speeds ever observed. Wind-driven current speed is known to be about 3% to 16% of the wind speed (Phillips and Groseva 1977). Constant R in Eq. 12 transforms the wind speed to wind-driven current speed and its value varies between 0.03 and 0.16. The other direction constants are given by equations similar to Eq. 12.

Equation 10 is the local CA rule and it is used to calculate the state of the (i,j) cell at time step t+1, i.e., the oil mass in the (i,j) cell at time step t+1, when the state of that cell and the states of its neighbours are known at time step t. Equation 10 describes also the effects of land areas, oil evaporation, and wind-driven and water currents on the state of the (i,j) cell at time step t+1. Wind-driven and water currents may be different in different cells and may vary with time. It should be stated here that Eq. 10 is not complete since some other factors such as water depth, coastal waves, shoreline deposition, and oil dissolution in water have not been included yet.

SIMULATION OF OIL SPILL MOVEMENT AND SPREADING

An algorithm for the simulation of oil slick movement and spreading, based on the model described in the previous section, has been developed in the framework of this research work. Figure 3 shows the

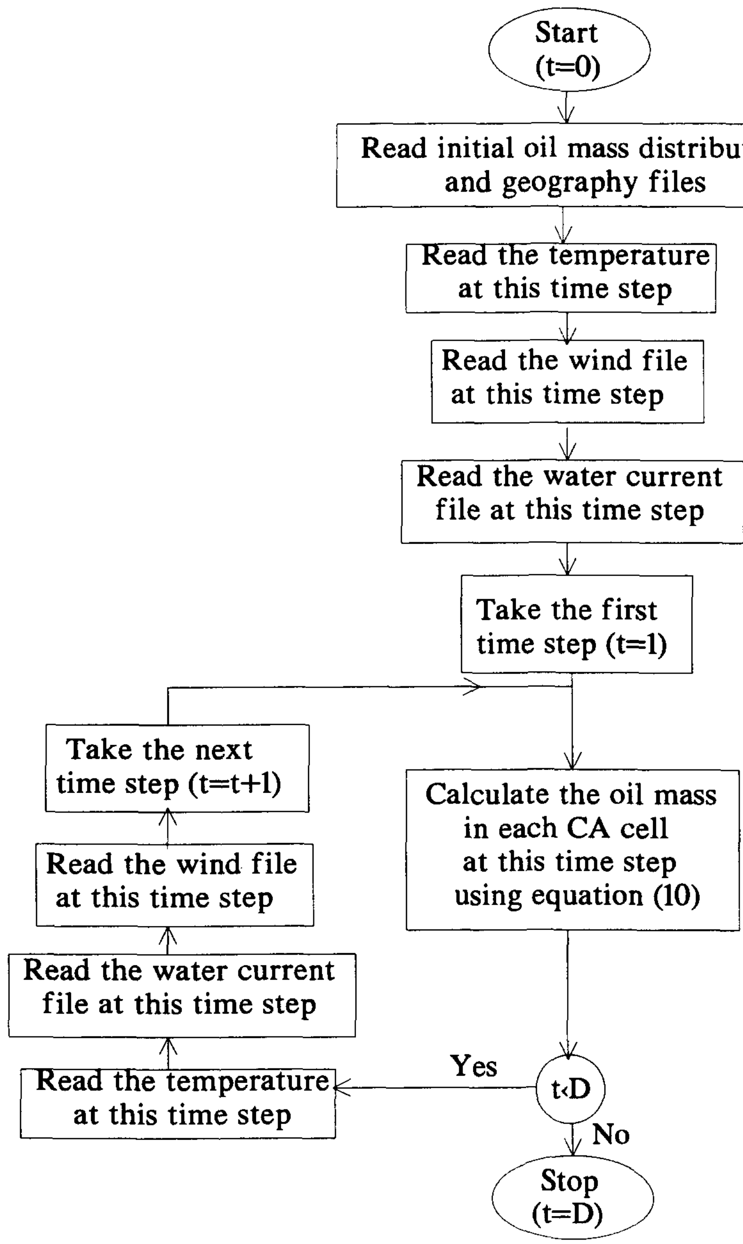

Fig. 3. The flow-chart of the algorithm.

flow-chart of the algorithm. The algorithm starts by setting the time step t equal to zero. Then the algorithm reads the initial oil mass distribution file, i.e., a two-dimensional matrix which has as elements the oil masses in each CA cell at time t=0, $M^0_{i,j}$. Then the algorithm reads the geography file, i.e., the two-dimensional matrix which has as elements the flags LF. After that, the algorithm reads the temperature of the environment at time t=0 and then the wind file which consists of two two-dimensional matrices containing the wind directions and speeds at each cell at time t=0, i.e., $WD^0_{i,j}$ and $WV^0_{i,j}$, and then reads the water current file which also consists of two two-dimensional matrices containing the water current directions and speeds at each cell at time t=0, i.e., $CD^0_{i,j}$, and $CV^0_{i,j}$. The algorithm takes the first step (t=1) and calculates the oil masses in each CA cell at time step t=1 using the CA local rule, i.e., Eq. 10. After that, the algorithm reads the temperature of the environment and the wind and water current files at time step t=1, takes the next time step t=2, and calculates the oil masses in each CA cell at time step t=2 using the CA local rule, and so on until the number of time steps becomes larger than a user defined constant D.

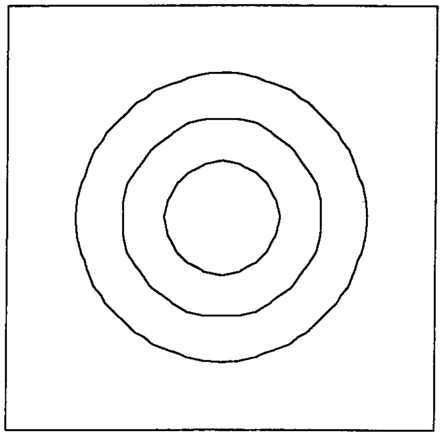

Fig. 4. The spreading of a circular oil slick in a square area were no land and no water currents exist and no winds blow.

The user of the algorithm is free to keep constant the temperature, wind and water currents in all time steps or to impose various temperatures, winds and water currents scenarios during the oil slick movement and spreading by altering the temperature and wind and water current files at any time step(s) she/he wishes.

Consider at time $t=t_1$ a hypothetical circular oil slick in a 10 km x 10 km square area shown in Fig. 4, where no land and no water currents exist and no winds blow. Suppose that the total oil mass is 50 000 kg and that the oil mass distribution in this circular oil slick follows a gaussian distribution, i.e., oil mass is maximum at the center of the slick and decreases with the circle radius following the Gaussian function. Suppose also that oil evaporation is essentially zero. The time step is defined by the user of the algorithm and, in this case, it was taken to be equal to 30 min. These characteristics of the oil slick and the value of the time step will be used throughout this section. In future times $t > t_1$, the algorithm should produce circular oil slicks all with the same center and with larger radius in larger times. This homogenous spreading is used to "calibrate" the algorithm, i.e., to determine the values of the constants m and d of Eq. 10. It was found that the algorithm produces circular slicks when the values of m and d are set to 0.0014 and 0.18, respectively. These values of m and d will be used throughout this section. Figure 4 shows the initial oil slick and its homogenous spreading, i.e., the slick at two future time steps, when the aforementioned values are used.

Consider at time $t=t_1$ the aforementioned hypothetical circular oil slick in a 10 km x 10 km square area, shown in Fig. 5. In this area, an arbitrarily shaped island is found. Suppose that no water currents exist

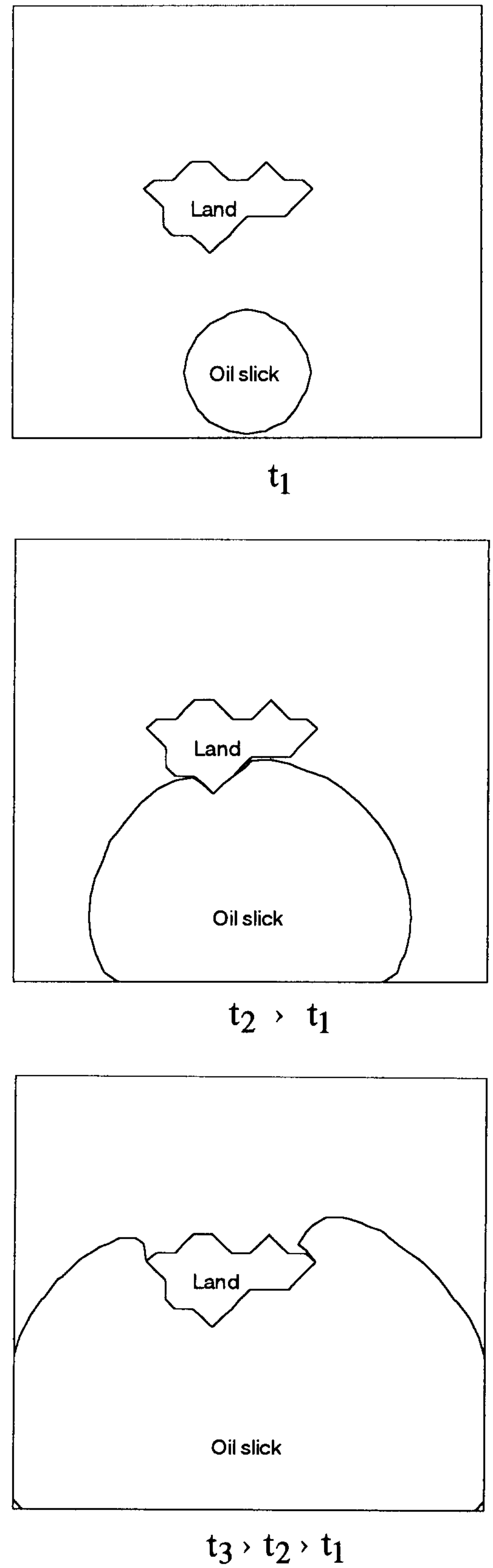

Fig. 5. Spreading of a circular oil slick in a square area with an arbitrarily shaped island ($t_3 > t_2 > t_1$). No water currents exist and no winds blow.

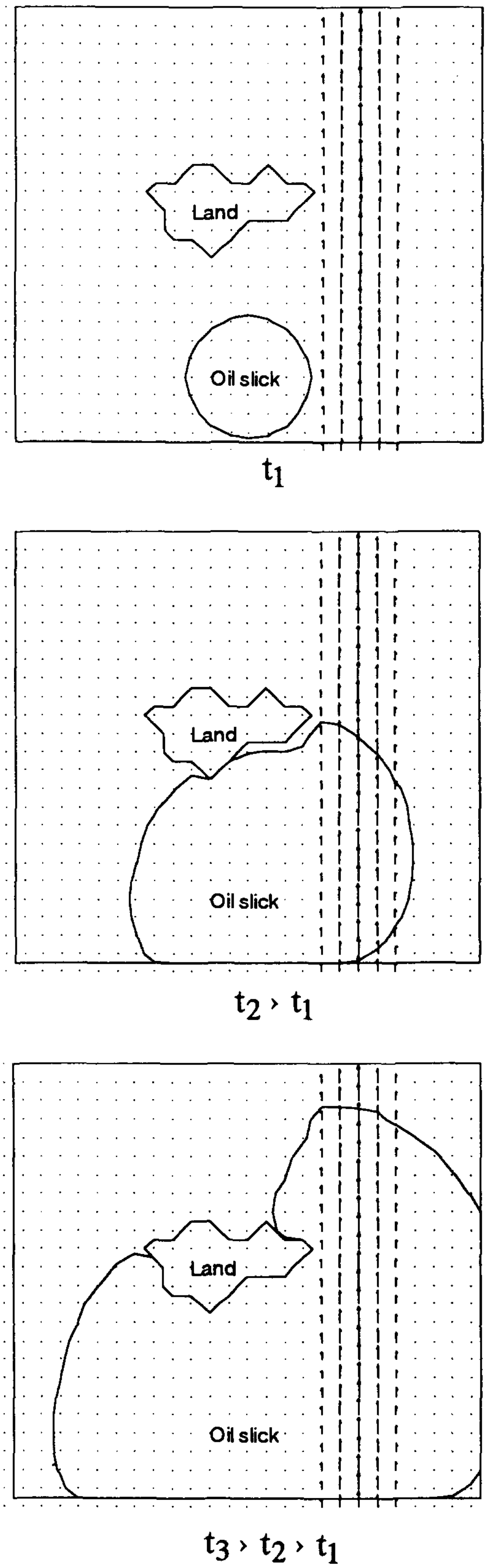

Fig. 6. Spreading and movement of a circular oil slick in a square area with an arbitrarily shaped island ($t_3 > t_2 > t_1$). A water current with direction from south to north exists. No winds blow.

and no winds blow. Figure 5 shows simulation results at two future times t_2 and t_3 ($t_3 > t_2 > t_1$). The oil slick spreads around the island.

Consider again, at time $t=t_1$, the same slick in the same area as in Fig. 5, but with a water current with direction from south to north as shown in Fig. 6. Suppose that no winds blow. The direction of the arrows in Fig. 6 shows the direction of the water current and the size of the arrows indicates the water current speed. The width of the water current strip is 1.5 km. The current speed at the center of the strip was taken to be equal to 20% of the maximum possible water current speed, whereas the speed at the edges of the strip was taken to be equal to 10%. The current speed was supposed to vary linearly from the center to the edges of the strip. The dots in Fig. 6 indicate that the current speed at these points is zero. Since no winds blow the wind-driven current speed is zero, i.e., Nw of Eq. 11 is equal to zero at all cells at all times. For cells corresponding to the center of the current strip, the values of the constants of Eq. 10 at all times are:

$$\begin{aligned} N^t_{i,j} &= -0.20 \\ E^t_{i,j} &= 0 \\ S^t_{i,j} &= 0.20 \\ W^t_{i,j} &= 0 \\ NE^t_{i,j} &= -0.05 \\ NW^t_{i,j} &= -0.05 \\ SE^t_{i,j} &= 0.05 \\ SW^t_{i,j} &= 0.05 \end{aligned} \tag{13}$$

For cells corresponding to the edges of the current strip, the values of the constants of Eq. 10 at all times are:

$$\begin{aligned} N^t_{i,j} &= -0.10 \\ E^t_{i,j} &= 0 \\ S^t_{i,j} &= 0.10 \\ W^t_{i,j} &= 0 \\ NE^t_{i,j} &= -0.01 \\ NW^t_{i,j} &= -0.01 \\ SE^t_{i,j} &= 0.01 \\ SW^t_{i,j} &= 0.01 \end{aligned} \tag{14}$$

The values of the constants of Eq. 10 for cells corresponding to areas between the center and the edges of the current strip vary linearly between the values of Eqs. 13 and 14. Figure 6 shows simulation results at two future times t_2 and t_3 ($t_3 > t_2 > t_1$). The effect of the water current becomes evident by comparing Figs. 5 and 6. The presence of the current increases the oil transport from south to north and causes a secondary oil transport from west to east.

Consider at time $t=t_1$ the aforementioned hypothetical circular oil slick in a 10 km x 10 km square area with no land in it, shown in Fig. 7. In this area, a water current exists. This current is the same as in Fig. 6 but its direction is from west to east. Suppose that in this area a wind blows. The direction of the wind is from south to north, its speed is taken to be equal to 50% of the maximum possible wind speed and the wind-driven current speed is taken to be equal to 10% of the wind speed. For cells corresponding to the center of the water current strip, the value of the constant $W^t_{i,j}$ at all times is:

$$W^t_{i,j} = Ww^t_{i,j} + Wc^t_{i,j} = 0 + 0.2 = 0.20 \quad (15)$$

and the value of the constant $S^t_{i,j}$ at all times is:

$$S^t_{i,j} = Sw^t_{i,j} + Sc^t_{i,j} = 0.05 + 0 = 0.05 \quad (16)$$

The values of the rest of the constants of Eq. 10 are obtained in a similar manner:

$$\begin{aligned} N^t_{i,j} &= -0.05 \\ E^t_{i,j} &= -0.20 \\ S^t_{i,j} &= 0.05 \\ W^t_{i,j} &= 0.20 \\ NE^t_{i,j} &= -0.06 \\ NW^t_{i,j} &= 0.04 \\ SE^t_{i,j} &= -0.04 \\ SW^t_{i,j} &= 0.06 \end{aligned} \quad (17)$$

For cells corresponding to the edges of the current strip, the values of the constants of Eq. 10 at all times are:

$$\begin{aligned} N^t_{i,j} &= -0.05 \\ E^t_{i,j} &= -0.10 \\ S^t_{i,j} &= 0.05 \\ W^t_{i,j} &= 0.10 \\ NE^t_{i,j} &= -0.02 \\ NW^t_{i,j} &= 0 \\ SE^t_{i,j} &= 0 \\ SW^t_{i,j} &= 0.02 \end{aligned} \quad (18)$$

The values of the constants of Eq. 10 for cells corresponding to areas between the center and the edges of the current strip vary linearly between the values

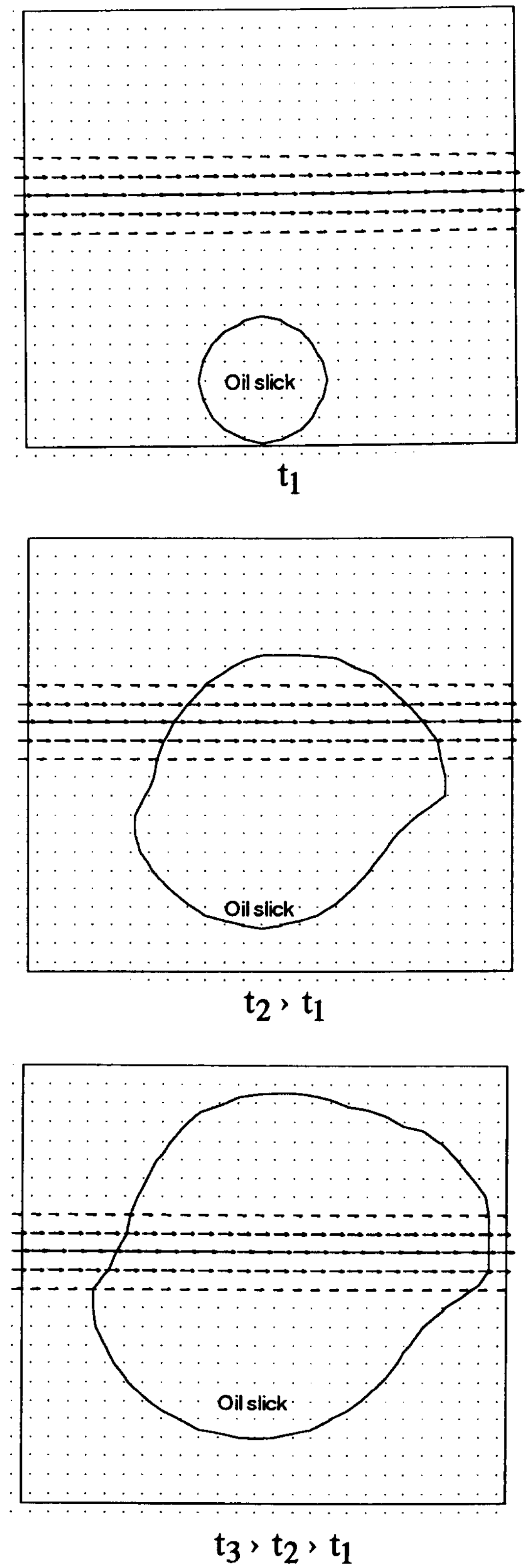

Fig. 7. Spreading and movement of a circular oil slick in a square area with no land in it ($t_3 > t_2 > t_1$). A water current with direction from west to east exists. A wind with direction from south to north blows.

of Eqs. 17 and 18. Figure 7 shows the combined effect of wind and water current on oil slick movement and spreading. This figure shows simulation results at two future times t_2 and t_3 ($t_3 > t_2 > t_1$).

CONCLUSIONS

A model for the prediction of oil slick movement and spreading using CAs was presented in this paper. The model is general and can predict the behaviour of oil slicks in regions with complicated boundaries. The effects of winds, surface currents, and oil evaporation are incorporated in this model. For the evaluation of the model, an algorithm for the simulation of oil slick movement and spreading has also been developed and used to simulate hypothetical oil slicks in hypothetical geographical regions. The results of the simulation are in qualitative agreement with real oil slick movement and spreading. Although the model is not yet complete, since some other factors such as water depth, coastal waves, shoreline deposition, and oil dissolution in water have not been included, it is evident that CAs are efficient in modelling such a complex and highly non-lin-ear phenomenon as oil slick movement and spreading.

REFERENCES

Adam, J.A. Specialties: Solar wings, oil spill avoidance, on-line patterns. IEEE Spectrum 32: 87-95; 1995.

Ages, A.B.; de Lange Boom, B.R.; Woodward, M.J. A drifter for tracking oil spills using the Argos system. In: Proc. OCEANS 94. Brest, France. New York, NY: IEEE Press 3; 1994: 292-297.

Alofs, D.J.; Reisbig, R.L. An experimental evaluation of oil slick movement caused by waves. J. Phys. Oceanogr. 2: 439-43; 1972.

Bass, F.G.; Puzenko, S.A. Detection of oil spills on the sea using radar measurements. J. Electromagn. Waves Appl. 8: 859-70; 1994.

Beer, T.; Humphries, R.B.; Bouwhuis, R. Modeling nearshore oil slick trajectories. Marine Pollut. Bull. 14: 141-4; 1983.

Capehart, B.L.; Welsh, L.W. Jr. Oil spill simulation in the Florida Gulf outer continental shelf. In: Proc. southeastern conf. '78. Atlanta, GA, USA. New York, NY: IEEE Publishing; 1978: 418-421.

Capehart, B.L.; Welsh, L.W. Jr. A computer simulation of oil spills. Simulation 33: 49-54; 1979.

Cekirge, H.M.; Sollohub, J.; Navon, I.M.; Nnaji, S. Models of oil spills in Florida waters. In: Proc. third international conference on development and application of computer techniques to environmental studies. Montreal, Canada. Southampton, UK: Comp. Mech. Publications; 1990: 357-62.

Cunningham, W.P.; Saigo, B.W. Environmental science. Dubuque, IA: Wm. C. Brown Publishers; 1995.

Easton, A.K. Oil spill modelling. In: Proc. eight biennial conference and bushfire dynamics workshop. Canberra, Australia. Canberra, Australia: Australian National University; 1989: 435-438.

El-sabh, M.I.; Murty, T.S. Simulation of the movement and dispersion of oil slicks in the Alabian Gulf. Natur. Hazards 1: 197-219; 1988.

Feynman, R.P. Simulating physics with computers. Int. J. Theor. Phys. 21: 467-88; 1982.

Gerhard, M.; Schuster, H. A cellular automaton describing the formation of spatially ordered structures in chemical systems. Physica D 36: 209-21; 1989.

Gerhard, M.; Schuster, H.; Tyson, J.J. A cellular automaton model of excitable media. Physica D 46: 392-415; 1990.

Gouveia, A.D.; Kurup, P.G. Probable movement of a hypothetical oil patch from the Bombay High region. Indian J. Marine Sci. 6: 118-21; 1977.

Gruner, K.; Reuter, T.; Smid, H. A new sensor system for airborne measurements of maritime pollution and hydrographic parameters. GeoJournal 24: 103-7; 1991.

Huhnerfuss, H.; Alpers, W.; Witte, F. Layers of different thickness in mineral oil spills detected by grey level textures of real aperture radar images. J. Remote Sensing 10: 1093-9; 1989.

Karafyllidis, I.; Thanailakis, A. Simulation of two-dimensional photoresist etching process in integrated circuit fabrication using cellular automata. Modell. Simul. Mater. Sci. Eng. 3: 629-42; 1995.

Karafyllidis, I.; Thanailakis, A. Simulation of the image reversal submicron process in integrated circuit fabrication. Semicond. Sci. Technol. 11: 214-20; 1996.

Karpen, J.; Galt, J. Modeling of oil migration in Puget Sound. In: Proc. OCEANS 79. San Diego, CA, USA. New York, USA: IEEE Press; 1979: 628-34.

Krapez, J.C.; Cielo, P. Optothermal evaluation of oil film thickness on water. J. Appl. Phys. 72: 1255-61; 1992.

Kurup, P.G. Oil slick trajectories for hypothetical spills in the Arabian Sea. Indian J. Mar. Sci. 12: 1-10; 1983.

Lehr, W.; Calhoun, D.; Jones, R.; Lewandowski, A. Model sensitivity analysis in environmental emergency management: A case study in oil spill modeling. In: Proc. winter simulation conference. Lake Buena Vista, FL. New York, NY: IEEE Publishing; 1994: 01198-205.

MacDonald, I.R.; Guinasso, N.L. Jr.; Ackleson, S.G.; Amos, J.F. Natural oil slicks in the Gulf of Mexico visible from space. J. Geophys. Res. 98: 16351-64; 1993.

Massin, J.M., ed. Remote sensing for the control of marine pollution. New York, NY: Plenum; 1984.

Matzke, D.J. Impact of locality and dimensionality limits on architectural trends. In: Proc. workshop on physics and computation, PhysComp'94, Los Alamitos, CA, USA. New York, NY: IEEE Computer Society Press; 1994: 30-35.

Minsky, M. Cellular vacuum. Int. J. Theor. Phys. 21: 537-51; 1982.

Neralla, V.R.; Venkatesh, S. Real-time application of an oil spill movement prediction system. Natur. Hazards 2: 31-44; 1989.

Okamoto, K.; Kobayashi, T.; Masuko, H.; Shimanta, M. Oil pollution detection experiments by the synthetic aperture radar on the European Remote Sensing Satellite-1. J. Commun. Res. Lab. 41: 161-4; 1994.

Okuyama, T.; Inomata, H.; Masuko H.; Nakamura, K. SIR-B experiments in Japan: Surface activity-oil-pollution experiment. J. Radio Res. Lab. 35: 39-54; 1988.

Omohundro, S. Modeling cellular automata with partial differential equations. Physica D 10: 128-34; 1984.

Omtzigt, E.T.L. Computational spacetimes. In: Proc. workshop on physics and computation, PhysComp'94. Los Alamitos, CA: IEEE Computer Society Press; 1994: 239-45.

Phillips, C.R.; Groseva, V.M. The spreading of crude oil spills across a lake. Water Air Soil Pollut. 8: 353-60; 1977.
Reijnhart, R.; Rose, R. Evaporation of crude oil at sea. Water Res. 16: 1319-25; 1982.
Toffoli, T. Cellular automata as an alternative to (rather than an approximation of) differential equations in modeling physics. Physica D 10: 117-27; 1984a.
Toffoli, T. CAM: A high-performance cellular automaton machine. Physica D 10: 195-204; 1984b
Vichniac, G.Y. Simulating physics with cellular automata. Physica D 10: 96-116; 1984.
von Neumann, J. Theory of self-reproducing automata. Urbana, IL: University of Illinois; 1966.
Weimar, J.R.; Tyson, J.J.; Watson, L.T. Diffusion and wave propagation in cellular automaton models of excitable media. Physica D 55: 309-27; 1992.
Wilding, N.B.; Trew, A.S.; Hawick, K.A.; Pawley, G.S. Scientific modeling with massively parallel SIMD computers. Proc. IEEE 79: 574-85; 1991.
Wolfram, S. Cellular automata and complexity. Reading, MA: Addison Wesley; 1994.
Yapa, P.D.; Hung Tao Shen; DeSheng Wang; Angammana, K. An integrated computer model for simulating oil spills in the upper St. Lawrence river. J. Great Lakes Res. 18: 340-51; 1992.
Zeigler, B.P. Discrete event models for cell space simulation. Int. J. Theor. Phys. 21: 573-88; 1982.